ANALYSIS OF ISOLATED PHOTONS IN PHOTOPRODUCTION IN PYTHIA

Andrii Iudin[1]*, Sergey Voronov[2]**

¹European Molecular Biology Laboratory, European Bioinformatics Institute
Hingston, Cambridge, United Kingdom
²National Technical University of Ukraine "Kyiv Polytechnic Institute named after Igor Sikorsky"
St. Polytechnic, 6, Kiev, Ukraine
*E-mail: andyyudin@gmail.com, **E-mail: s.voronov@kpi.ua

Collision of particles at high energies at accelerators is the main source of data used to obtain deeper understanding of the fundamental interactions and the structure of the matter. Processes of isolated photon production have provided many tests of theoretical descriptions of the universe on scales smaller than the proton. This work is dedicated to the analysis of the large amount of collision data that has been accumulated at ZEUS in 2004-2007 period and new methods of processing isolated photons that have been proposed. The authors develop software algorithms that allow obtaining the signal of isolated photons from the data collected on the ZEUS detector at electron-proton collider HERA, calculating the differential cross sections, and comparing the measured data with PYTHIA Monte Carlo predictions. Taking into account the features of the ZEUS detector, the photon signal is separated from the background events and the number of isolated photons is calculated. Computational mathematical and numerical methods have been used to simulate the interaction of particles in the detector. Monte Carlo predictions for differential cross sections as functions of the pseudorapidity and transverse energy of the photon η^γ, E_T^γ and the jet η^{jet}, E_T^{jet}, and the fraction of the photon momentum x_γ^{meas} carried by the interacting parton have been calculated and compared with the experimental data. The results of the study are compared with the previous studies and show for the first time that all isolated photon HERA measurements are consistent with each other. New results show improved uncertainties. The formation of isolated inclusive photons and photons with the accompanying jet was measured in photoproduction with ZEUS detector at HERA collider using the integrated luminosity of 374 ± 7 pb⁻¹. For the first time, more complex Monte-Carlo simulation models of isolated photons for ZEUS detector were generated and applied, and the description of the photon signal was improved. It has been found that PYTHIA describes the shape of the cross section as a function of η^γ well enough, but does not fully reproduce the shape of E_T^γ, E_T^{jet}, and the middle region of x_γ^{meas}, while η^{jet} is described not very well. The reason for this discrepancy can be the lack of corrections of higher orders in the predictions for cross sections of direct photons. Scaling of the cross sections obtained with PYTHIA improves the description of E_T^γ and η^γ. The unsatisfactory description of η^{jet} indicates that further studies are required.

KEYWORDS: isolated photons, photoproduction, jet, Monte Carlo, PYTHIA, the electron-proton collision

Recently, high-energy particle collisions at accelerators have been the main source of experimental data used to gain a deeper understanding of the properties of fundamental interactions and to reveal the structure of matter. There are many different facilities for conducting such studies. Among them are ring and linear accelerators. Some experiments study the frontal collision of particles (colliders), but there are some that consider the collision of particles with a fixed target. In particular, HERA electron-proton ring collider (Hadron-Elektron-Ringanlage) is a great place to test many aspects of quantum chromodynamics (QCD), a fairly successful field theory describing interactions between fundamental components. Protons were accelerated to an energy of 920 GeV and electrons (positrons) to 27.5 GeV, corresponding to the centre of mass energy of 318 GeV. This paper is devoted to the study of data collected during the ZEUS experiment at the HERA collider.

The results of the fundamental interaction between subatomic particles that occur over a very short period of time in a well-localized region of space (so-called events) can be classified by measuring the particles that appear in the final state. One such event category is isolated photon events [1]. Some of Feynman diagrams for the formation of isolated photons are shown in Fig. 1. Circles indicate that the target has a structure, for example, a quark from a proton interacts, while the remnant of the proton is shown at a broad arrow. Similarly, for the photon.

In the kinematic region at HERA, the direct non-fragmentation process for the formation of isolated photons is mainly the QCD Compton process [2] (Fig. 1 (a)) $\gamma q^p \rightarrow \gamma q$, where q^p denotes the quark structure of the proton. The input photon interacts with the quark in the proton. In the final state observed, there is a photon with a large transverse momentum and a jet with a large transverse momentum. The contribution of this process to the cross section is of an order of $O(\alpha_{em}^2)$, where α_{em}^2 is the electromagnetic coupling constant.

Resolved non-fragmentation process has three processes (Fig. 1 (b)):

$$q^\gamma g^p \rightarrow \gamma q, \qquad q^\gamma \bar{q}^p \rightarrow \gamma g, \qquad g^\gamma q^p \rightarrow \gamma q,$$

where q^γ denotes the quark composition of the photon.

In principle, resolved isolated photon processes are able to show the distribution of not only quarks, but also gluons in the photon. However, the kinematic coverage available in this analysis has less sensitivity to the distribution of gluons in the photon. The magnitude of the hard scatter is of the order $O(\alpha_{em}^2 \alpha_s)$, where α_s is the constant of the strong coupling.

But after taking into account the factor $O(\alpha_{em}/\alpha_s)$ for the structure of the photon, the cross section is of the order of $O(\alpha_{em}^2)$, similarly as for the direct process.
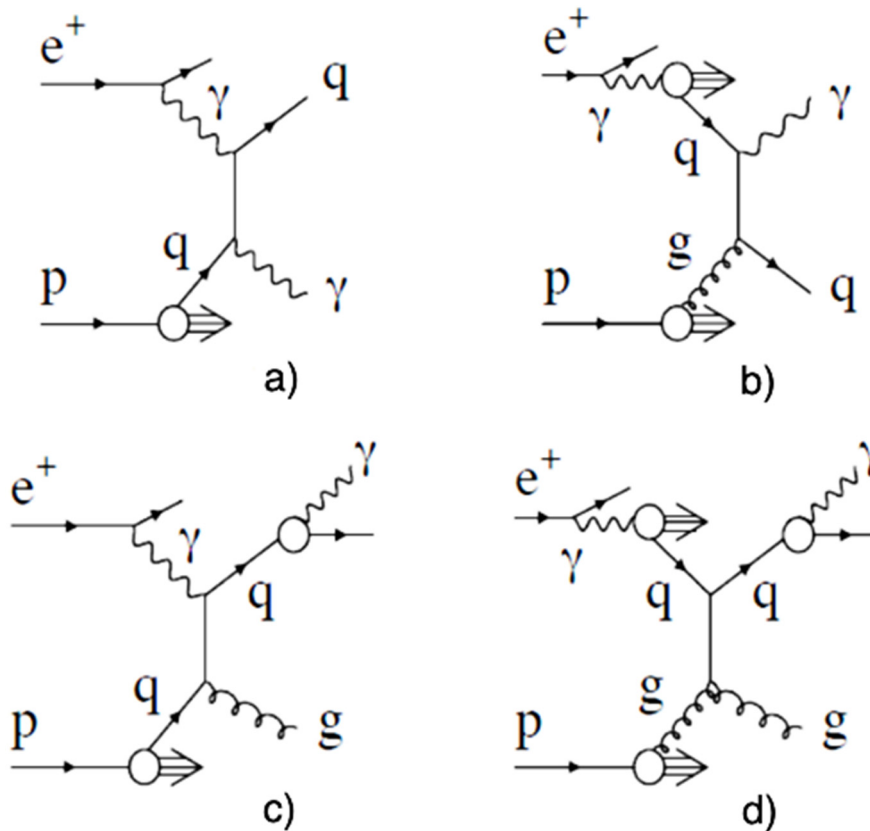

Fig. 1. Basic leading order QCD diagrams for isolated photons:
a) direct non-fragmentation; b) resolved non-fragmentation; c) direct fragmentation; d) resolved fragmentation

An isolated photon may also emerge from jet fragmentation. Thus, the diagrams that are contributing to the cross section are the same as for the two-jet process. Direct and resolved fragmentation processes: $\gamma q^p \to qg$, $q^\gamma g^p \to qg$ are shown in Fig. 1 (c, d). The next factor for photon fragmentation is given as $O(\alpha_{em}/\alpha_s)$. After taking into account the fragmentation factor and the photonic structure, the cross section is $O(\alpha_{em}^2)$ for direct and resolved fragmentation processes. Since cross section of fragmentation processes depends on fragmentation functions, its contribution decreases sensitivity to the measured distribution of partons in the photon. If such a photon takes almost all of the energy of the initial quark, then the event may be experimentally similar to that of the non-fragmentation process. After taking into account the isolation criterion, events of this nature will be referred to as isolated photon fragmentation events. The requirement of isolation reduces their contribution to the measured cross-section [3].

Despite the relatively low frequency of isolated photon events, background events that give distortion in the measured spectra can also occur. The main background is provided by neutral mesons with high transverse momentum, such as π^0, η mesons, which can decay into two photons formed in the process of jet fragmentation. In order to reduce the proportion of such background events, the isolation cone around the isolated photon in the coordinates (η, φ) is used in the experimental data. But even after using isolation, there is still a fraction of background events in the data. Due to the large cross section of jet formation, the fraction of background from neutral mesons is approximately equal to the fraction of signal – true isolated photons. This part of the background events is subtracted by statistical methods.

The research of photons has one significant advantage compared to many other studies of high-energy particles that are born in collisions, the photons are stable and so are measured in the detector unchanged since they were emitted from the colliding particles. Thus, the photon carries information directly from the collision, regardless of other processes. Other elemental particles that can be released by collisions may not exist in isolation. Instead, they undergo a fragmentation process in which other particles are formed, which also fragment until the resulting particles are able to form stable bound states. These stable particles are then observed in the detector. The existence and properties of the original particle are derived from these particle decays. This can increase uncertainties.

The study of isolated photon events is useful for testing theoretical understanding of the structure of matter on a scale smaller than a proton in experiments with a fixed target and colliding beams at HERA and others. Experiment ZEUS published results of first observations of isolated photons with accompanying jets at high transverse momenta

conducted at luminosity of 6.4 pb^{-1} [1]. ZEUS collaboration also published work on measuring the production of isolated photons in deep inelastic *ep* scattering [4]. Isolated photons in deep inelastic *ep* scattering were measured using the ZEUS detector at HERA using an integrated luminosity of 320 pb^{-1}. Measurements were made in ranges of the transverse energy and the pseudo-rapidity of the isolated photon $-4 < E_T^\gamma < 15$ GeV and $-0,7 < \eta^\gamma < 0.9$ for the virtuality of the exchanged photons, Q^2, in the range $10 < Q^2 < 350$ GeV^2 and invariant masses of the hadron system $W_X > 5$ GeV. Parton showers that were simulated with Monte Carlo methods, gave quite a good description of the data on most of the kinematic range. Predictions of Gehrmann-De Ridder et al. [5-7] of order α^3 reproduced the shapes of the experimental results as functions of the transverse energy and the pseudorapidity, but lay lower than the measurements at low Q^2 and low x. The predictions of Martin et al. [8] are mainly below the cross sections that are measured, but close in kinematic regions where lepton radiation is expected to be dominant. Improved data description can be obtained by combining the two corresponding predictions, which raised questions about the need for further calculations fully using the potential measurements. Work of H1 collaboration investigated prompt photons without and with a requirement of an accompanying jets in photoproduction at HERA [9]. The processes of *ep* collisions with the energy of the centre of mass 319 GeV on the detector H1 at HERA with the corresponding integrated luminosity of 340 pb^{-1} were studied. Cross sections were measured for photon and jet transverse energies greater than 6 GeV and less than 15 GeV and a pseudorapidity between -1.0 and 2.4. The differential cross sections were reconstructed as functions of the transverse energy, the pseudorapidity, x_γ and x_p. The correlation between the jet and the photon was also investigated. The results are compared with the predictions of theory, based on the collinear approach and the k_T-factorization approach. The predicted cross sections are usually underestimating the data by 20%. Both predictions underestimate measurements at low E_T^γ. Form of the cross section as a function of pseudorapidity of photons is best described with the k_T-factorization approach and as functions of other studied variables are fairly well described within the error. However, theorists still had the task of improving the description. Recently it was established that k_T-factorization model and leading order QCD describe well isolated photons in deep inelastic scattering [10, 11]. The comparison of the experimental data with theoretical models was also conducted without trying to correct the predictions generated in PYTHIA to results at the level of partons [12].

FORMULATION OF THE PROBLEM

The purpose of this work is to develop algorithms for obtaining with a high precision the signal of isolated photons from the sample of data collected by the ZEUS detector at the electron-proton collider HERA during 2004-2007 period [13, 14], calculate the differential cross sections using this signal and compare them with predictions of Monte Carlo simulations (MC).

EXPERIMENT AND KINEMATIC SPACE

Investigated data were collected with the ZEUS detector [15] and correspond to the integrated luminosity of 374 pb^{-1} [13, 14]. The high-precision uranium calorimeter of the ZEUS detector made it possible to perform measurements within the pseudorapidity between -0.74 and 1.01. The smallest unit that can independently read in the calorimeter is called a cell. The cells are organized into layers and towers. The cells of the inner layer of each section are called cells of the electromagnetic calorimeter. They have the fine detail required to separate electromagnetic charges and extract prompt photon signal.

Differential cross sections as a function of several variables were measured in the kinematic region determined in the laboratory system of reference as: virtuality of the exchange photon $Q^2 < 1$ GeV^2, inelasticity of the interaction $0.2 < y_{JB} < 0.7$, pseudorapidity of the photon $-0.7 < \eta^\gamma < 0.9$, transverse energy of the photon $6 < E_T^\gamma < 15$ GeV, and, when a jet was required, transverse energy of the jet $4 < E_T^{jet} < 15$ GeV and pseudorapidity of the jet $-1.5 < \eta^{jet} < 1.8$.

MONTE CARLO EVENT GENERATION

The generation of MC events for the case of *ep* scattering for models and methods used in this paper divides into a set of sequential steps:

• **Hard scattering.** The interaction between particles is described by matrix elements calculated in accordance with Feynman rules. This perturbative step defines the main characteristics of the event. The proton parton is selected according to the parton distribution function (PDF), which describes the probability of finding the parton in the proton by the values of Q^2 and the variable Bjorken x. Photon PDF is used to select the parton of the photon in the case of a resolved event.

• **Radiation of the initial and final states.** The presence of charged or colored objects before or after hard interaction can lead to large corrections related to photonic or gluon radiation. The electromagnetic radiation is modelled according to the theory of quantum electrodynamics. The quantum chromodynamics corrections can be modelled with the so-called model of parton showers (PS) [16] that describes the parton cascade by splitting one parton into two. Possible transitions $q \to qg$, $g \to q\bar{q}$, $g \to gg$. The PS model can be used for the the initial and final state radiation and, therefore, the particle that takes part in the hard interaction may already be derived from the separation of the partons.

An alternative to the PS model is the color dipole model [17], where each pair of colored objects is treated as gluons emitting colored dipoles. The radiation leads to additional radiating dipole gluons as a result of the parton cascade. In the case of *ep*-scattering, the cascade is initiated by a dipole built up by the quark that is struck and the proton residue.

• **Fragmentation.** After the radiation step, as the distances between partons increase, the QCD becomes strongly interacting – and the perturbation theory is broken. Colored partons are combined into colorless hadrons in the fragmentation process. Since the fragmentation region is not perturbative, some phenomenological models are used.

In the Lund string model [18, 19] two color-charged objects are linked together to form a string. As the two particles move away from each other, the potential energy of the string increases until enough energy is accumulated to produce a quark-antiquark pair due to the rupture of the string. The newly created quarks are connected to the free ends of the outgoing string and the process continues until there are stable hadrons.

Alternative to the Lund string models is provided by the model of fragmentation of cluster decay [20]. With this approach, all the gluons in the parton shower break into quark-antiquark pairs. Colorless $q\bar{q}$ pairs form clusters that then break up into hadrons in the final state.

• **Detector simulation.** In the last step, the particles in the final state are passed through the detector simulation to allow the simulation of the detector response. Detector modelling for ZEUS is performed in MOZART (MC for ZEUS analysis, reconstruction and triggers) [21], based on the GEANT program [22] developed by CERN. The properties of the event can be investigated with the help of partons, hadrons or objects of the detector, i.e., particles can be viewed at three levels: parton, hadron and detector.

The parton (generator) level takes into account all particles after the fragmentation step. The hadron level uses all stable particles in the final state formed in the fragmentation step, as well as stable particles that do not undergo hadronisation. In this work, we used a model with the generation of a jet that fragmented into a photon and a jet, and with the generation of particles such as π^0 and η mesons that are forming photons. Finally, the experimentally measured detector level uses all objects obtained after the reconstruction stage, such as tracks and clusters. A direct comparison between data and theory is only possible at one, as a rule, hadron level. As the MC should be represented at all three levels, it can be in used for comparison of calculations on different levels [13,14].

MONTE CARLO SAMPLES

Ten MC samples were obtained for the specified particular purposes in this analysis. For the generation of MC samples, the generator PYTHIA [23, 24] (version 6.221 and 6.416) was used. The formation of events is based on the elements of the scattering matrix for the processes listed in Tables 1 and 2. The choice of these processes is based on the fact that they correspond to the photoproduction of isolated photons studied in this work. PYTHIA calculates parton showers and uses JETSET [25] to simulate the fragmentation of Lund strings. Multiparton interaction is realized by adding interaction between parton-observers in the same event. Generated sample consisted of 951.03 pb^{-1} direct events and 3525.06 pb^{-1} resolved. When choosing PDF in this work it was necessary to take into account the particularities of ZEUS detector and the existing software for the simulation of events measuring with this detector (MOZART, CZAR - Complete ZGANA Analysis Routine, ZEPHYR - ZEUS physics analysis, EAZE - Easy Analysis of ZEUS Events) [21, 26]. Therefore, in both cases, the proton PDF is CTEQ4M [27] and the photon is GRVHO [28, 29].

To get the signal from the measured data most of MC events were generated in PYTHIA that worked in the channel of prompt photon with codes of direct and resolved subprocesses (ISUB) as shown in the Table 1. In addition, the radiated photons, both in the direct and resolved mode, are selected from the two-jet MC sample obtained with the subprocesses shown in Table 2 with hard photon emission in the final state. Namely, these are the processes of photon-lepton - Compton scattering, prompt photons, point photons in the photoproduction and QCD jet. Here f_i means a fundamental fermion of flavor i, q_i – quark, g – gluon and γ – photon. In hadron colliders, the ISUB = 14 and 29 processes provide the main source for the formation of single photons. According to Fig. 1 (a) for ISUB = 34 we have a reaction between the quark (f_i) from the proton and the photon (γ) from the positron that creates quark (f_i) and photon (γ). In the same way we have, for example, in Fig. 1 (b) ISUB = 29 where gluon and quark form a photon and quark. Similarly, Table. 2 lists the processes depicted in Fig. 1 (c, d).

Table 1

The processes included in the generation of non-fragmentation signal PYTHIA MC

Direct ISUB process		Resolved ISUB process	
34	$f_i\gamma \to f_i\gamma$	14	$f_i\bar{f_i} \to g\gamma$
		18	$f_i\bar{f_i} \to \gamma\gamma$
		29	$q_ig \to q_i\gamma$

EAZE [30] is the basis for code analysis and provides a standard format that simplifies the process of writing code. There are two important parts to the design from a user perspective. The first one is the control card file. This file can make various preliminary calls to select the data to be processed by making changes to the standard control charts. This

allows general code guidance. The second part of the user code is called in three stages. Initially, the code is customized, and all the necessary statements are made. Then begins the second part, which runs on each of the data selections.

Table 2
The processes included in the generation of fragmentation signal and background PYTHIA MC

Direct ISUB process		Resolved ISUB process	
33	$f_i\gamma \rightarrow f_i g$	11	$f_i f_j \rightarrow f_i f_j$
54	$g\gamma \rightarrow f_k \overline{f}_k$	12	$f_i \overline{f}_i \rightarrow f_k \overline{f}_k$
		13	$f_i \overline{f}_i \rightarrow gg$
		28	$f_i g \rightarrow f_i g$
		53	$gg \rightarrow f_k \overline{f}_k$
		68	$gg \rightarrow gg$

Most cuts and the preliminary analysis are performed at this point. In the end some final requirements are applied. ORANGE – ROOT [31] for analysis [30] is a program that works within EAZE. ORANGE does, however, have a more detailed set of control charts that use standard code and code that is centrally supported to get started analysing the information. This significantly reduces the amount of time it takes to generate the analysis code, and because the code is centrally maintained, it increases the reliability of the code used.

In this analysis, ORANGE was used to perform pre-selection events and reject deliberately bad events.

SIGNAL EXTRACTION

After the pre-selection provided by ZEUS, there are still some non-*ep* and other background events that are removed by the following conditions:

- -40 cm < Z_{vertex} < 40 cm – the vertex of interaction along the 0Z axis (i.e., along the proton direction) should be in a well-understood region.

- Barrel calorimeter (BCAL) [15] timing less than 10 ns rejects events of sparks of photo-electron multipliers (PEM).

- The transverse momentum P_T must be at least 10 GeV.

BCAL timing is a useful tool for deleting spark and cosmic events. If the time registered in BCAL is very far from the time of the event, then it can be assumed that the energy deposit is not associated with *ep* collision. A timing of 10 ns was chosen after modelling the PYTHIA Monte Carlo program in the previous ZEUS analysis.

Cosmic events, for example, often have a large amount of missing P_T, so that they do not occur from the colliding beams and they are found mainly in the up-down direction (i.e., the axis 0Y).

Events, generated by PEM sparks or charged flux events, where neutrino takes the place of the scattered electron, are also rejected with a cut on the missing P_T. False positive events, which are generated by PEM sparks and background beam gas are also reduced by the BCAL timing cut.

The following cuts were used to obtain a clean sample of photoproduction events:

- If an event has a candidate for deep inelastic scattering (DIS) electron in SINISTRA [32, 33] with a probability of more than 90% and y_{el} < 0.7, then such event is removed from the final stack of candidate events for photon.

- 0.2 < y_{JB} < 0.7

A method that has been well established in other ZEUS publications [34-36] has been used here as well. The lower boundary y_{JB} discards any proton gas residues and other background events, such as cosmic events. The upper limit removes DIS events as well as events that include a lepton that was mistakenly identified as a prompt photon.

For photon finding the use of the so-called free procedure of clustering is recommended, such as k_T clustering algorithm [3, 37] to identify isolated photons. Past ZEUS collaboration articles on isolated photons [4] have applied a k_T clustering algorithm to ZUFO (ZEUS Unidentified Flying Object) [38] to reconstruct candidates for isolated photons as a k_T jet. Therefore, in this analysis the selection of photon signal is carried out by means of reconstruction of candidate for photon by k_T clustering isolation of ZUFO. The ZUFO method defined the photon as the only ZUFO. Isolation was performed according to the requirements so that ZUFO candidate for the photon had at least 90% energy of k_T jet in which he was clustered.

- Pseudorapidity of the candidate is requires such that it was in the acceptance of ZEUS BCAL, where shower shapes are well understood: 0.7 < η^γ < 0.9.

- The upper bound on E_T^γ is motivated by the level of understanding of the shower shapes and the decrease of the signal at high transverse energies. The lower limit is set due to poor energy resolution at low energies: 6 < E_T^γ < 15 GeV.

- By requiring that at least 90% of the energy of a candidate for the photon is stored in electromagnetic calorimeter layer, we reduce the hadron background: $F_{EMC} = E_{EMC} / E_{tot} > 0.9$, where E_{EMC} – the energy in the electromagnetic calorimeter layer, E_{tot} – the total measured energy.

Isolation is performed using the variable Z_{KT}, which is defined as:
$$Z_{KT} = E_\gamma / E_{jet},$$
where E_γ is the ZUFO energy of the photon candidate and E_{jet} is the energy of the k_T jet in which the candidate was clustered. A study of the Frixione isolation [39] and its subsection – conical isolation was also carried out.

Cone isolations is determined by using a variable Z_{cone}, that is the candidate energy E divided by E_{cone} - the total energy in the η - φ cone with a radius of 1.0 around the candidate (including the energy of the candidate itself), i.e.,
$$Z_{cone} = E_\gamma / E_{cone}$$
- For the study of different isolations, the following cut was used: $Z_{cone} > 0.9$.

Stephano Frixione proposed a form of isolation that, as he claims, would remove fragmentation events. The idea is to use not only one cone, but concentric series of cones with radius $\rho \leq \rho_0$ such that inside such cone, total E_T is less than function $\chi(\rho) = E_\gamma \, \epsilon_\gamma ((1 - \cos(\rho))/(1 - \cos(\rho_0)))^n$. The simple cone algorithm considers one cone $\rho_0 = 1$ and $\epsilon_\gamma = 0.1$. A satisfactory discrepancy within the error range between the results of using different isolations was found. Due to the fact, that in this analysis Frixione method and simple cone isolation does not provide a significant benefits we use the following cut: $Z_{KT} > 0.9$.

- Also, the requirement that there was no track in 0.2 units in $\eta - \varphi$ was used: $\Delta Rtrack > 0.2$,

where $\Delta Rtrack = \sqrt{\left(\eta_\gamma - \eta_{track}\right)^2 + \left(\varphi_\gamma - \varphi_{track}\right)^2}$

- The tracks had to have a transverse momentum $p > 250$ MeV. This reduction also discards electrons and other charged background.

The jets are clustered with the k_T algorithm [3]. Preliminary analysis of the prompt photons in ZEUS uses cone algorithm grounded on the definition of jets in which the jet made up of all the particles, which are inside the cone in $\eta - \varphi$. However, this algorithm is not infrared safe (i.e., the observables depend on the physics of low-energy/large distances), and therefore, in case if the particles in the jets emit a large amount of soft (i.e., with low E_T) particles, the number of found jets and their properties will be different.

Prompt photon events can be viewed in an inclusive form and with an accompanying jet requirement. In the latter case, the jets must undergo a selection of cuts of $4 < E_T^{jet} < 35$ GeV and $-1.5 < \eta^{jet} < 1.8$.

To further separate the photon signal from the background of neutral mesons π^0 and η a variable $\langle \delta Z \rangle$ is used, which is defined as:

$$\langle \delta Z \rangle = \sum_i |Z_i - Z_{cluster}| / (w_{cell} \sum_i E_i),$$

where Z_i is the Z position of the center of cell i, $Z_{cluster}$ - the cluster center, w_{cell} - the width of the cell in Z direction, E_i energy recorded in the cell and the sum is done by all cells in the cluster. The distributions $\langle \delta Z \rangle$ for MC photons and background π^0 and η mesons, as defined in the selection procedure, are shown in Fig. 2. Here, the solid line denotes the photon signal and the dotted line is the background of the neutral mesons π^0 and η.

There is a noticeable peak in photon distribution at about ~ 0.1, which corresponds mainly to the showers contained in a single cell. Then there is a "shoulder" up to ~ 0.6, where the photon falls close to the center of the cell and splits its energy into two cells, or the photon undergoes early pair formation (preshower). Next, note the small peak at ~ 0.5, where the photon hits the boundaries of the cells and spreads its energy evenly to two adjacent in Z cells or where e^+e^- from the conversion of the photon hit adjacent in Z cells.
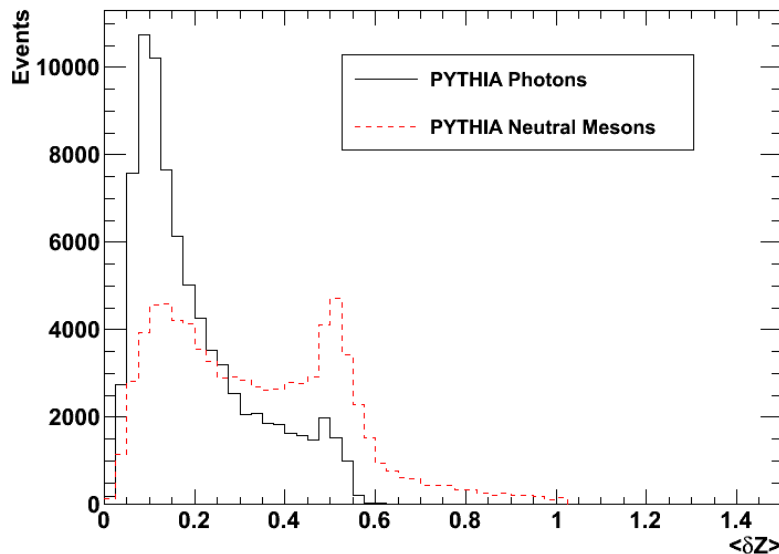

Fig. 2. Comparison of the $\langle \delta Z \rangle$ distribution in MC for signal of photoproduction
of resolved and direct photon with background from neutral mesons π^0 and η

The background curve has a small peak in the region $0.1 < <\delta Z> < 0.2$ with a further noticeable peak centered at $<\delta Z> = 0.5$. The first peak is the result of π^0 decay with an angle close to the minimum that will hit the calorimeter with similar values of Z, thus giving a narrow width in Z. The peak at 0.5 is a geometric effect in which two photons from π^0 decay strike cells adjacent to Z, distributing their energies equally between the two cells, giving a width of 0.5. At large $<\delta Z>$ the tail disappears shortly after 0.5 (by analogy with the distribution of photons), because if the decay photons fall on non-adjacent cells, they will be reconstructed as two separate objects.

Thus, applying the least squares method to the distribution of $<\delta Z>$ by statistical subtraction of the background we can derive from the data N_{SIG} – the number of signal events.

CALCULATION OF CROSS SECTIONS

The full cross section is calculated by the equation:

$$\sigma = 1/L * N_{SIG}/A,$$

where σ is the cross section, L is the integrated luminosity, and N_{SIG} is the number of signal events observed at the detector level, which is modified to account for the detector loss using the MC-based evaluation of the acceptance factor, which gives the total number of signal events.

Cross sections are presented differentiated in bins (i.e., subintervals) of transverse energy and pseudorapidity of the photon $E_T{}^\gamma$ and η^γ and the jet $E_T{}^{jet}$, η^{jet}, and the fraction of the momentum of the photon $x_\gamma{}^{meas}$ which is being carried by the interacting parton

$$x_\gamma{}^{meas} = \frac{E^\gamma + E^{jet} - p_Z^\gamma - p_Z^{jet}}{E^{all} - p_Z^{all}},$$

where E^γ, E^{jet} – photon and jet energies, p_Z – the corresponding longitudinal momentum, "all" denotes all particles measured in the event in the final state.

For any bin ΔY variable Y (it could be E_T^γ and η^γ, E_T^{jet}, η^{jet} or x_γ^{meas}) the differential cross section with respect to the Y, $d\sigma/dY$, is given as

$$d\sigma/dY = 1/\Delta Y * 1/L * N_{SIG} * C,$$

where N_{SIG} and L are calculated for events in the range ΔY, and C is the factor of acceptance correction:

$$C = 1/A.$$

COMPARISONS WITH PREVIOUS MEASUREMENTS

The differential cross sections as a function of η^γ, measured in a defined phase space, are shown in Fig. 3. The ZEUS data of this work are shown in black squares, the previous ZEUS results [40] are blue and H1 results [9] are red. The measured phase spaces are not identical to the ZEUS HERA-I measurements and the H1 HERA-II publication; the current ZEUS measurement has a cut of $-0.7 < \eta^\gamma < 0.9$, while the H1 measurement has a cutoff of $-1.0 < \eta^\gamma < 2.4$. Previous ZEUS measurements use cone-based isolation and have a lower cut-off at $E_T{}^\gamma > 4$ GeV, whereas H1 and current ZEUS measurements are 6 GeV. For all given points, the internal error lines are statistical uncertainties, and the outer error lines represent statistical and systematic squared errors. ZEUS points are offset for clarity of comparison of form dependency.
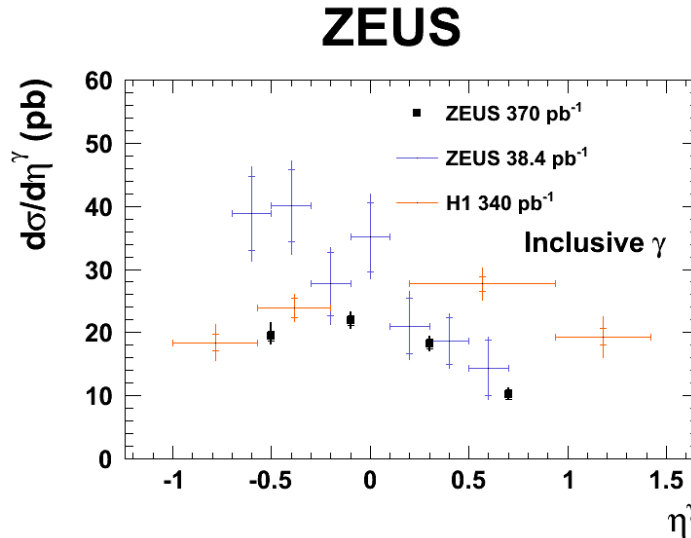

Fig. 3. Differential inclusive cross section of isolated photons as a function of η^γ within a defined kinematic region in comparison with previous HERA measurements.

It is clear that all HERA measurements show a decrease in cross section with increasing pseudorapidity, and all measurements agree with one another within errors and taking into account different binning and slightly different kinematic regions. The new ZEUS results presented here demonstrate significantly improved uncertainties. Both statistical and systematic errors were smaller than in the previous ZEUS results compared to the H1 uncertainties, especially given the broader H1 bins.

COMPARISONS WITH THE MONTE CARLO MODEL

Differential cross sections using full phase space are shown for inclusive photons for η^γ and E_T^γ in Fig. 4 and for photons with the requirement of an accompanying jet for η^γ, E_T^γ, η^{jet}, E_T^{jet} and x_γ^{meas} in Fig. 5. As before, the measured ZEUS cross sections are shown in black squares and the internal error lines show statistical uncertainty and the outer error lines are statistical and systematic errors squared. In addition, MC model predictions are shown. Uncertainty of results of the modelling originating from dependence of cross sections of events, which are calculated in the generator PYTHIA, on scales of renormalisation and factorization have been found sufficiently small to be neglected. PDFs were not varied due to the specifications of the modelling of the ZEUS system in MOZART, CZAR and others. That is, this study follows the established practice regarding the uncertainties of MC [41, 42].
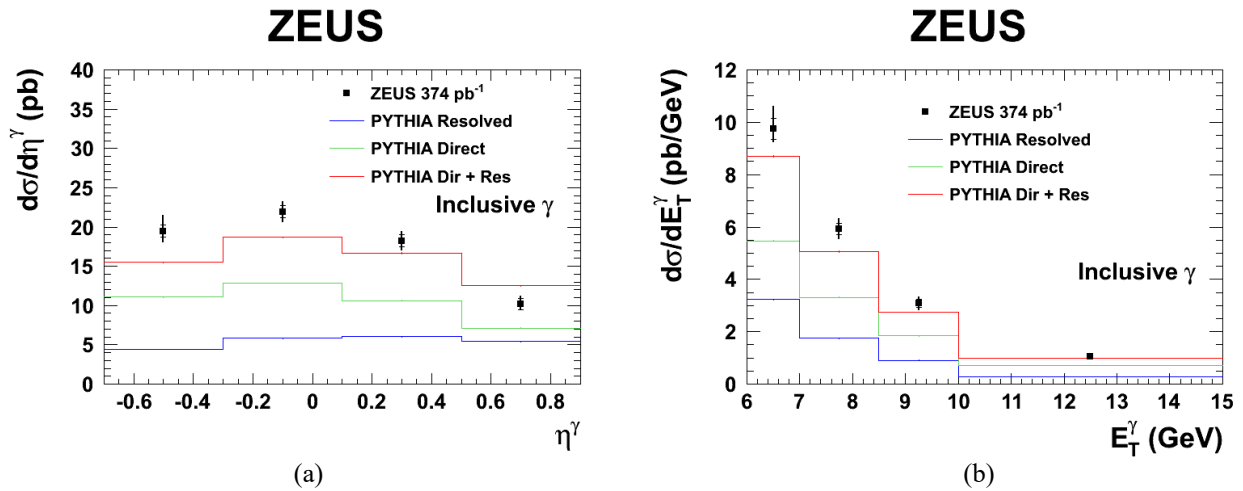

Fig. 4. Differential inclusive cross sections of isolated photons as a functions of η^γ (a) and E_T^γ (b), compared with MC predictions
(for the legend see the text)

The prediction for cross sections of production of resolved photons, which is obtained from PYTHIA 6.416, is shown as blue histogram. Contribution of a direct photon (green histogram) is also estimated with PYTHIA 6.416. As can be seen from previous results [43], the simple sum of PYTHIA predictions for direct photons with the MC prediction for resolved photons is significantly underestimating the measured data. Thus, the PYTHIA predictions are normalized to the overall normalization of the MC in a way to fit the data. This overall MC prediction (resolved plus direct) is shown as a solid red line.

Fig. 4 depicts distributions for an inclusive isolated photon. In Fig. 4 (a) a slowly falling cross section with increasing pseudorapidity of the photon is shown, which is described reasonably good by the combined MC prediction. For ZEUS data, the differential cross section shown in Fig. 4 (b) depends on the transverse energy approximately as:

$$d\sigma/dE_T^\gamma = 3797.48 * (E_T^\gamma)^{-3.18}$$

This is well modelled by MC, although the prediction of MC a bit underestimates E_T^γ.

Fig. 5 depicts distributions for an isolated photon with the requirement of an accompanying jet. In Fig. 5 (a) we see again a slowly declining cross section with an increase in the pseudorapidity of a photon, which is well described by the combined prediction of MC. The differential cross section as a function of E_T^γ is shown in Fig. 5 (b). It shows a dependence of form similar to that in Fig. 4 (b). Both the E_T^γ and η^γ distributions in the case of an accompanying jet are described by the MC better than in the case of an inclusive photon. In Fig. 5 (c) shows the cross section as a function of the pseudorapidity of the jet, which is not well described by the combined prediction of MC for small and large η^{jet}. The differential cross section as a function of the energy of the jet E_T^{jet} for ZEUS is shown in Fig. 5 (d) and is described by the MC as well as in the case of E_T^γ. In Fig. 5 (e) a steeply rising cross section with increasing x_γ^{meas} is shown, which is very well described by a combined prediction. The theoretical calculations are influenced by the parton processes that contain contributions of perturbation theory of QCD beyond the leading order. Discussion of these uncertainties, as well as the contributions of processes higher than the leading order in the perturbation theory of QCD in the study of the phase space specified in this work was carried out earlier [13, 14].
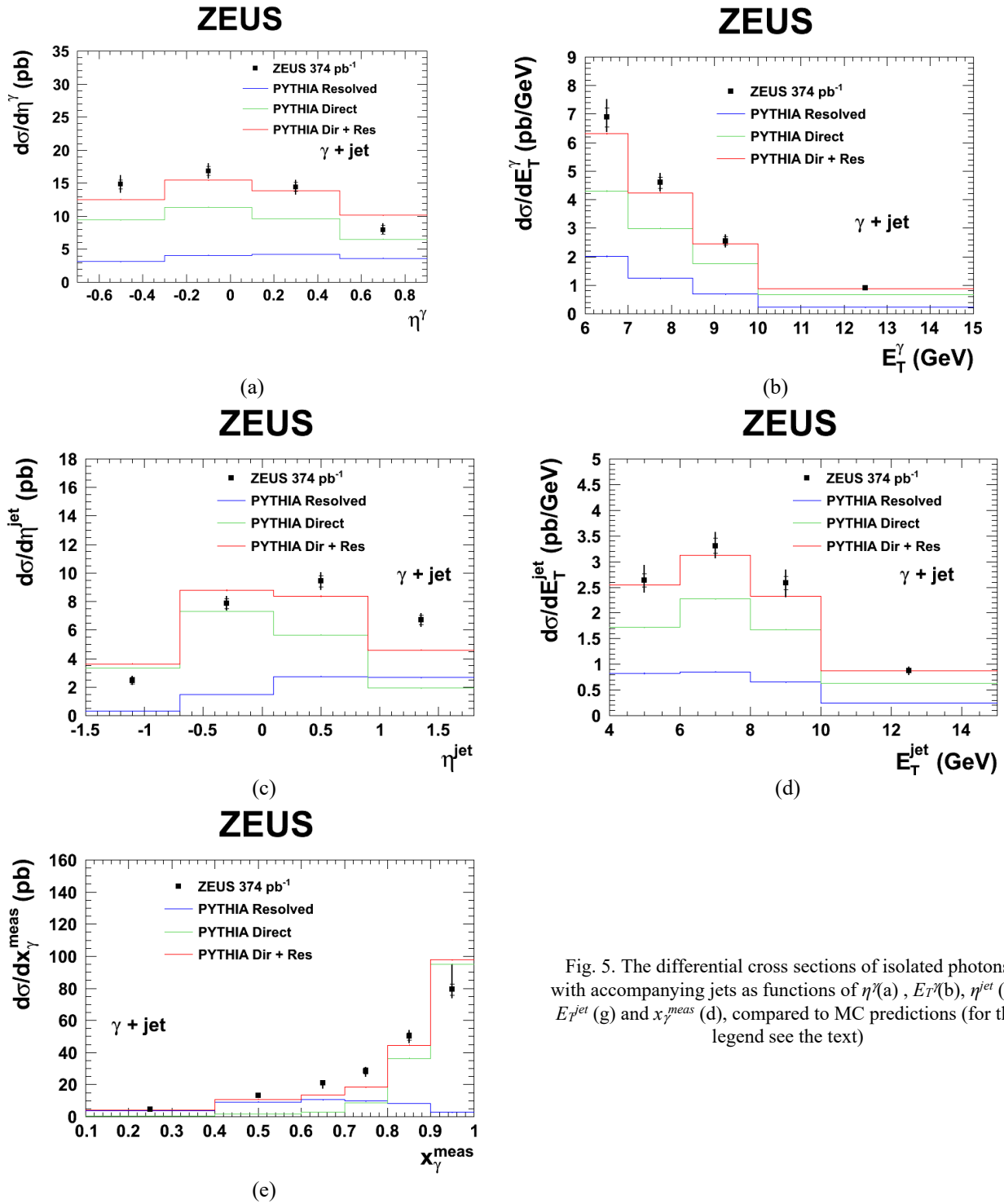
ZEUS

(a)

ZEUS

(b)

ZEUS

(c)

ZEUS

(d)

ZEUS

(e)

Fig. 5. The differential cross sections of isolated photons with accompanying jets as functions of η^γ(a), E_T^γ(b), η^{jet} (c), E_T^{jet} (g) and x_γ^{meas} (d), compared to MC predictions (for the legend see the text)

CONCLUSIONS

The inclusive isolated photons and photons with an accompanying jet were measured in photoproduction with the ZEUS detector at HERA accelerator using the integrated luminosity of 374 ± 7 pb^{-1}. These results improved past ZEUS results that were made with lower integrated luminosity. Past publication by ZEUS group dedicated to prompt photons in photoproduction used the data measured with the ZEUS detector at HERA accelerator during 1999-2000. These data corresponded to the integrated luminosity of 77 pb^{-1} [44].

More sophisticated MC simulation samples were generated and applied, unlike in previous studies, where samples were generated for only one particle. The description of the photon signal has been improved. MC predictions underestimate the measured cross sections by a significant amount. One of the reasons for this discrepancy may be the absence in the calculation of contributions of higher orders in perturbation theory of QCD. Uncertainties of results of

modelling that originate from dependency of cross sections, which are calculated in the PYTHIA events generator, on scales of renormalisation and factorization and variations of PDFs are not considered.

Scaling the prediction from the PYTHIA MC generator by a factor of 1.8 is required to normalize the MC to the measured cross sections. After such scaling, the shapes of differential cross sections for variables of the scattered photons, E_T^γ and η^γ, are well described. Also, within the error the shapes of the differential cross sections as functions of variables for events with a jet E_T^{jet}, η^{jet} and x_γ^{meas} are described by MC program, except for large values of η^{jet}, which indicates that further investigation is required.

In the field of isolated photons in *ep*-scattering many possibilities for further studies remain, both in theory and in experiment. These results will be useful for conducting and preparing experiments at future accelerators. The next step may be to improve the existing software system ZEUS (MOZART , ZEPHYR , EAZE etc.) with the latest PDFs such as CT14 [45].

ORCID IDs

Andrii Iudin https://orcid.org/0000-0002-1118-2853, **Sergey Voronov** https://orcid.org/0000-0002-0053-0381

REFERENCES

[1]. J. Breitweg, et al., Physics Letters B **413** (1), 201-216 (1997).
[2]. P. Newman and M. Wing, Rev.Mod.Phys. **86** (3), 1037 (2014).
[3]. S. Catani, et al., Nuclear Physics B, **406** (1), 187-224 (1993).
[4]. H. Abramowicz, et al., Physics Letters B, **715** (1), 88-97 (2012).
[5]. A. Gehrmann-De Ridder, G. Kramer, and H. Spiesberger, Nuclear Physics B, **578**(1), 326-350 (2000).
[6]. A. Gehrmann-De Ridder, T. Gehrmann, and E. Poulsen, Physical Review Letters, **96**(13), 132002 (2006).
[7]. A. Gehrmann-De Ridder, T. Gehrmann, and E. Poulsen, The European Physical Journal C - Particles and Fields, **47**(2), 395-411 (2006).
[8]. S.P. Baranov, A.V. Lipatov and N.P. Zotov, Phys.Rev. **D81**, 094034 (2010).
[9]. F.D. Aaron, et al., The European Physical Journal C, **66**(1), 17-33 (2010).
[10]. O. Hlushchenko, PoS, **DIS2017**, 177 (2018).
[11]. H. Abramowicz, et al., Journal of High Energy Physics, **2018**(1), 32 (2018).
[12]. PJ Bussey, CERN Proceedings, **1**, 175 (2018).
[13]. H. Abramowicz, et al., Phys.Lett. **B730**, 293-301 (2014).
[14]. H. Abramowicz, et al., Journal of High Energy Physics, **2014**(8), 23 (2014).
[15]. A.S. Yudin, O.T. Bogorosh and S.O. Voronov, Наукові вісті НТУУ «КПІ» [Scientific News of NTUU "KPI"], **2(94)**, 110–116 (2014).
[16]. M. Bengtsson and T. Sjöstrand, Zeitschrift für Physik C Particles and Fields, **37** (3), 465-476 (1988).
[17]. G. Gustafson, Physics Letters B, **175**(4), 453-456 (1986).
[18]. B. Andersson, et al., Phys.Rept. **97**, 31-145 (1983).
[19]. B. Andersson, G. Gustafson, and B. Söderberg, Zeitschrift für Physik C Particles and Fields, **20**(4), 317-329 (1983).
[20]. GC Fox and S. Wolfram, Nuclear Physics B, **168**(2), 285-295 (1980).
[21]. T. Haas, and *ZEUS-Note 92-021* (1992).
[22]. J. Allison, et al., Nuclear Instruments and Methods in Physics Research Section A: Accelerators, Spectrometers, Detectors and Associated Equipment, **835**, 186-225 (2016).
[23]. T. Sjöstrand, et al., Computer Physics Communications, **135**(2), 238-259 (2001).
[24]. T. Sjöstrand, S. Mrenna, and P. Skands, Journal of High Energy Physics, **2006**(05), 026 (2006).
[25]. T. Sjöstrand, Computer Physics Communications, **82**(1), 74-89 (1994).
[26]. R. Gläser, and *ZEUS-Note 90-114* (1990).
[27]. HL Lai, et al., Physical Review, D **55**(3), 1280-1296 (1997).
[28]. M. Glück, E. Reya, and A. Vogt, Physical Review, D **46**(5), 1973-1979 (1992).
[29]. M. Gluck, E. Reya, and A. Vogt, Z.Phys. **C48**, 471-482 (1990).
[30]. ZEUS Collaboration, (2013), Vol. 2013. Retreived from: http://www-zeus.desy.de.
[31]. I. Antcheva, et al., Computer Physics Communications, **180**(12), 2499-2512 (2009).
[32]. H. Abramowicz, A. Caldwell and R. Sinkus, Nuclear Instruments and Methods in Physics Research Section A: Accelerators, Spectrometers, Detectors and Associated Equipment, **365**(2), 508-517 (1995).
[33]. R. Sinkus and T. Voss, Nuclear Instruments and Methods in Physics Research Section A: Accelerators, Spectrometers, Detectors and Associated Equipment, **391**(2), 360-368 (1997).
[34]. H. Abramowicz, et al., Journal of High Energy Physics, **2013**(5), 97 (2013).
[35]. H. Abramowicz, et al., Journal of High Energy Physics, **2013**(5), 23 (2013).
[36]. H. Abramowicz, et al., Journal of High Energy Physics, **2013**(9), 58 (2013).
[37]. SD Ellis and DE Soper, Phys.Rev. **D48**, 3160-3166 (1993).
[38]. N. Tuning, and *Internal ZEUS Note* (2001), pp. 1-18.
[39]. S. Frixione, Physics Letters B, **429**(3), 369-374 (1998).
[40]. J. Breitweg, et al., Physics Letters B, **472**, 175-188 (2000).
[41]. M. Aaboud, et al., The European Physical Journal C, **79**(3), 205 (2019).
[42]. T. Yang, EPJ Web Conf. **60**, 14005 (2013).
[43]. FD Aaron, et al., The European Physical Journal C, **54**(3), 371-387 (2008).
[44]. S. Chekanov, et al., The European Physical Journal C, **49**(2), 511-522 (2007).
[45]. S. Dulat, et al., Phys.Rev. **D93** (3), 033006 (2016).

АНАЛІЗ ІЗОЛЬОВАНИХ ФОТОНІВ У ФОТОНАРОДЖЕННІ В PYTHIA
А.С. Юдін[1], С.О. Воронов[2]
[1]European Molecular Biology Laboratory, European Bioinformatics Institute
Хінкстон, Кембридж, Велика Британія
[2] Національний технічний університет України «Київський політехнічний інститут імені Ігоря Сікорського»
вул. Політехнічна, м. Київ, Україна

Зіткнення частинок при високих енергіях на прискорювачах є основним джерелом даних, що використовуються для отримання більш глибокого розуміння фундаментальних взаємодій і структури речовини. Дана робота присвячена аналізу великої кількості даних зіткнень, накопичених на ZEUS у 2004-2007 роках, та запропонованим новим методам розрахунку ізольованих фотонів. Автори розробили програмні алгоритми, що дозволяють отримувати сигнал ізольованих фотонів з даних, зібраних на детекторі ZEUS на електронно-протонному коллайдері HERA, обчислити диференціальні перерізи та порівняти виміряні дані з Монте Карло передбаченнями PYTHIA. Враховуючи особливості детектора ZEUS, фотонний сигнал відокремлюється від фонових подій і обчислюється кількість ізольованих фотонів. Для моделювання взаємодії частинок у детекторі використовувалися обчислювальні математичні та чисельні методи. Розраховано та порівняно з експериментальними даними передбачення Монте Карло моделі диференціальних перерізів як функції псевдобистроти та поперечної енергії фотону η^γ, E_T^γ та струмення η^{jet}, E_T^{jet} та частки імпульсу фотона x_γ^{meas} яку несе партон, що взаємодіє. Результати дослідження порівнюються з попередніми дослідженнями і вперше показують, що всі HERA вимірювання узгоджуються одне з одним. Нові результати показують покращену невизначеність. Утворення ізольованих інклюзивних фотонів і фотонів із супроводжуючим струменем було виміряне в фотонародженні детектором ZEUS на прискорювачі HERA з використанням інтегральної світності 374±7 пб[-1]. Вперше було згенеровано та застосовано більш складні зразки Монте Карло симуляції ізольованих фотонів для детектора ZEUS та покращено опис сигналу фотонів. Встановлено, що PYTHIA досить добре описує форму перерізу як функцію η^γ, але не повністю відтворює форму E_T^γ, E_T^{jet} і та середній проміжок x_γ^{meas}, тоді як η^{jet} описується не дуже добре. Причиною такої розбіжності може бути відсутність виправлень вищих порядків у передбаченнях перерізів прямих фотонів. Масштабування перерізів, отриманих за допомогою PYTHIA, покращує опис E_T^γ і η^γ. Незадовільний опис η^{jet} свідчить про необхідність подальших досліджень.
КЛЮЧОВІ СЛОВА: ізольовані фотони, фотонародження, струмінь, Монте Карло, PYTHIA, електрон-протонне зіткнення

АНАЛИЗ ИЗОЛИРОВАННЫХ ФОТОНОВ В ФОТОРОЖДЕНИИ В PYTHIA
А.С. Юдин[1], С.А. Воронов[2]
[1]European Molecular Biology Laboratory, European Bioinformatics Institute
Хинкстон, Кембридж, Великобритания
[2]Национальный технический университет Украины «Киевский политехнический институт имени Игоря Сикорского»
ул. Политехническая, 6 г. Киев, Украина

Столкновения частиц при высоких энергиях на ускорителях являются основным источником данных, используемых для более глубокого понимания фундаментальных взаимодействий и структуры вещества. Процессы рождения изолированных фотонов обеспечили множество тестов теоретического описания вселенной на масштабах меньших, чем протон. Эта работа посвящена анализу большого количества данных столкновений, накопленных на ZEUS в период 2004-2007 гг. и новым предложенным методам расчётов изолированных фотонов. Авторы разработали программные алгоритмы, которые позволяют получать сигнал изолированных фотонов из данных, собранных на детекторе ZEUS на электрон-протонном коллайдере HERA, вычислять дифференциальные сечения и сравнивать измеренные данные с Монте Карло предсказаниями PYTHIA. Принимая во внимание особенности детектора ZEUS, фотонный сигнал отделяется от фоновых событий и рассчитывается количество изолированных фотонов. Для моделирования взаимодействия частиц в детекторе были использованы вычислительные математические и численные методы. Рассчитано и сравнительно с экспериментальными данными предсказания Монте Карло модели дифференциальных сечений как функции псевдобыстроты и поперечной энергии фотона η^γ, E_T^γ и струи η^{jet}, E_T^{jet}, и доли импульса фотона x_γ^{meas}, которую несет взаимодействующий партон. Результаты исследования сравниваются с предыдущими исследованиями и впервые показывают, что все измерения HERA изолированных фотонов согласуются друг с другом. Новые результаты показывают улучшение неопределенности. Образование изолированных инклюзивных фотонов и фотонов с сопутствующей струей было измерено в фоторождении с помощью детектора ZEUS на коллайдере HERA с использованием интегральной светимости 374 ± 7 пб[-1]. Впервые были созданы и применены более сложные образцы Монтеn Карло симуляций изолированных фотонов для детектора ZEUS, а также улучшено описание фотонного сигнала. Было установлено, что PYTHIA достаточно хорошо описывает форму поперечного сечения как функцию от η^γ, но не полностью воспроизводит форму E_T^γ, E_T^{jet} и среднюю область x_γ^{meas}, тогда как η^{jet} описывается не очень хорошо. Причиной такого несоответствия может быть отсутствие поправок более высоких порядков в предсказаниях для сечений прямых фотонов. Масштабирование сечений, полученных с помощью PYTHIA, улучшает описание E_T^γ и η^γ. Неудовлетворительное описание η^{jet} указывает на необходимость дальнейших исследований.
КЛЮЧЕВЫЕ СЛОВА: изолированные фотоны, фоторождение, струя, Монте Карло, PYTHIA, электрон-протонное столкновение